SISSA

Experimental ion mobility measurements in Ne-N$_2$

To cite this article: A.F.V. Cortez *et al* 2016 *JINST* **11** P11019

View the article online for updates and enhancements.

You may also like

Experimental ion mobility measurements in Ne-N$_2$

A.F.V. Cortez,[a,b,1] **P.M.C.C. Encarnação,**[a,b] **R. Veenhof,**[c,d] **P.N.B. Neves,**[e] **F.P. Santos,**[a,b] **F.I.G.M. Borges**[a,b] **and C.A.N. Conde**[a,b]

[a]*Laboratory of Instrumentation and Experimental Particle Physics – LIP,*
 Rua Larga, 3004-516 Coimbra, Portugal

[b]*Department of Physics, Faculty of Science and Technology, University of Coimbra,*
 Rua Larga, 3004-516 Coimbra, Portugal

[c]*RD51 collaboration, CERN,*
 Genève, Switzerland

[d]*Department of Physics, Uludağ University,*
 16059 Bursa, Turkey

[e]*Closer Consultoria, LDA,*
 Lisboa Codex, Portugal

 E-mail: andre.f.cortez@gmail.com

ABSTRACT: Data on ion mobility is important to improve the performance of large volume gaseous detectors, such as the ALICE TPC or in the NEXT experiment. In the present work the method, experimental setup and results for the ion mobility measurements in Ne-N$_2$ mixtures are presented. The results for this mixture show the presence of two peaks for different gas ratios of Ne-N$_2$, low reduced electric fields, E/N, 10–20 Td (2.4–4.8 kV·cm^{-1}·bar^{-1}), low pressures 6–8 Torr (8–10.6 mbar) and at room temperature.

---

[1]Corresponding author.

Contents

1 Introduction

Measuring the mobility of ions in gases is relevant in several areas from physics to chemistry, e.g. in gaseous radiation detectors modelling and in the understanding of the pulse shape formation [1, 2], and also in IMS (Ion Mobility Spectrometry) a technique used for the detection of narcotics and explosives [3]. In order to fully understand and model these detectors it is important to have detailed information on the transport properties of ions.

Using the experimental method described in detail in [4], the mobility of ions in neon-nitrogen (Ne-N$_2$) gas mixtures is measured at pressures in the 6 to 8 Torr (8 to 10.6 mbar) range and for reduced electric fields commonly used in gaseous detectors, 15 Td (3.6 kV·cm^{-1}·bar^{-1}), extending previous studies developed in our group for other gases [4–13].

1.1 Ion mobility

Under a weak and uniform electric field a group of ions will eventually reach a steady state characterized by a drift velocity [3], v_{d}, expressed by:

$$v_{\mathrm{d}} = KE \tag{1.1}$$

where K is the mobility of the ions, expressed in units of cm^2·V^{-1}·s^{-1} and E the intensity of the drift electric field. The ion mobility, K, is normally expressed in terms of reduced mobility K_0,

$$K_0 = KN/N_0 \tag{1.2}$$

where N is the gas number density and N_0 is the Loschmidt number ($N_0 = 2.6867 \times 10^{19}$ cm^{-3}). The mobility values can be presented as a function of the reduced electric field E/N in units of Townsend (1 Td=10^{-17} V·cm^2).

1.2 Langevin's theory

According to Langevin's theory [14], one limiting value of the mobility is reached when the repulsion becomes negligible compared to the polarization effect. This limit is given by the following equation,

$$K_{\text{pol}} = 13.88 \left(\frac{1}{\alpha \mu} \right)^{\frac{1}{2}} \tag{1.3}$$

where α is the neutral polarisability in cubic angstroms ($\alpha = 0.394$ Å^3 for Ne [15] and $\alpha = 1.74$ Å^3 for N$_2$ [15]) and μ is the ion-neutral reduced mass in atomic mass units. The Langevin limit is the value of K in the double limit of low E/N and low temperature, conditions which ensure the dominance of the polarization attraction over other atomic interactions (e.g. hard sphere repulsion), describing well our experimental conditions: low pressure, low temperature and low reduced electric fields.

1.3 Blanc's law

In binary gaseous mixtures Blanc's law has proven to be most useful when determining the ions' mobility. According to this law the reduced mobility of the ion in the binary mixture, K_{mix}, can be expressed as follows:

$$\frac{1}{K_{\text{mix}}} = \frac{f_1}{K_{g1}} + \frac{f_2}{K_{g2}} \tag{1.4}$$

where K_{g1} and K_{g2} are the reduced mobility of that same ion in an atmosphere of 100% of gas #1 and #2 respectively and f_1 and f_2 are the molar fraction of each gas in the binary mixture [16].

2 Method and experimental setup

The mobility measurements presented in this study were obtained using the experimental system described in [4]. A UV flash lamp with a frequency of 10 Hz emits photons that impinge on a 250 nm thick CsI film deposited on the top of a GEM that is inside a gas vessel. The photoelectrons released from the CsI film trigger an electron avalanche inside the GEM holes, where they ionize the gas molecules encountered along their paths. While the electrons are collected at the bottom of the GEM electrode, the cations formed will drift across a uniform electric field region towards a double grid; the first acts as Frisch grid while the second, at ground voltage, collects the ions' charge. A pre-amplifier is used to convert the charge collected into a voltage signal, and the time spectra are recorded in a digital oscilloscope. After the background is subtracted from the signal, gaussian curves are fitted to the time of arrival spectra from which the peak centroids are obtained. Since the peaks' centroid corresponds to the average drift time of the ions along a known distance, the drift velocity and mobility can then be calculated. One important feature of the method is the capability of controlling the voltage across the GEM (V_{GEM}), and so the energy gained by the photoelectrons as they move across the GEM holes. This characteristic proves to be a great advantage since it enables the identification of the primary ions based on their ionization energies. Identifying the primary ions will allow to pinpoint secondary reaction paths that lead to the identification of the detected ions.

Since impurities play an important role in the ions' mobility, before each experiment the vessel was vacuum pumped down to pressures of 10^{-6} to 10^{-7} Torr and a strict gas filling procedure was

carried out. No measurement was considered until the signal stabilised, and all measurements were done in a 2–3 minutes time interval to ensure minimal contamination of the gas mixture, mainly due to outgassing processes.

The method described together with the knowledge of the dissociation channels, product distribution and rate constants represent a valid, although elaborate, solution to the ion identification problem.

3 Results and discussion

The mobility of the ions originated in Ne-N_2 mixtures have been measured for different reduced electric fields E/N (from 10 Td up to 20 Td) and different pressures (in the 6–8 Torr pressure range) at room temperature (298 K).

The range of the reduced electric field values used to determine the ions' mobility is limited due to two distinct reasons: one is the electric discharges that occur at high E/N values; the other is the observed deterioration of the time of arrival spectra for very low values of E/N (below 5 Td or 1.2 kV·cm^{-1}·bar^{-1}), which has been attributed to collisions between the ions and impurity molecules.

A background work on the mobilities and ionization processes of Ne [5] and N_2 [6] in their parent gases has already been performed in our group.

3.1 Ne-N_2 mixture

In neon-nitrogen (Ne-N_2) mixtures with N_2 concentrations higher than 10% only one peak is observed, as can be seen in figure 1. The ion responsible for this peak is the same ion as in pure N_2 according to the cross sections and rate constants displayed in table 1, i.e. N_4^+. Since the total ionization cross section for electron impact (at an energy of 23 eV) in Ne is 0.0166±0.001×10^{-16} cm^2 [17] — about 18 times lower than that for N_2 (0.492±0.025×10^{-16} cm^2 [18])), it is expected that even at low N_2 concentrations (down to about 5% of N_2), N_2 ions are still the ones preferentially produced. For N_2 concentrations below 10% in the mixture another peak becomes visible as can be observed in figure 1. In table 1 the possible reactions are summarized together with the respective ionization cross sections or rate constants.

Figure 2 shows the evolution of the fraction of ion species present as a function of time for N_2 concentration of 10% (figure 2a), and 50% (figure 2b), for a total pressure of 8 Torr. The relative abundance of the different ion species was calculated using both electron impact ionization cross sections and the reaction rates summarized in table 1.

As can be seen, the fraction of the different ion species present at the end of the drift distance will depend on the reaction time. A careful analysis of figure 2 can help to explain figure 1, where the time-of-arrival spectra for several Ne-N_2 mixtures (5%, 10%, 50% and 90% of N_2) at a pressure of 8 Torr, temperature of 298 K and for a reduced electric field of 15 Td with a voltage across GEM of 23 V, are displayed. As can be inferred from table 1, at very low N_2 concentrations (up to about 5% of N_2), the production of Ne$^+$ ions will be more abundant, leading to the same ions as in pure Ne, while above this and up to 10% of N_2, both Ne and N_4^+ ions will be produced.

Observing figure 2a, at the instant corresponding to the detected ions' drift time taken from the peaks's centroid of figure 1 (10% N_2), about 0.15 ms, it is possible to conclude that the ions
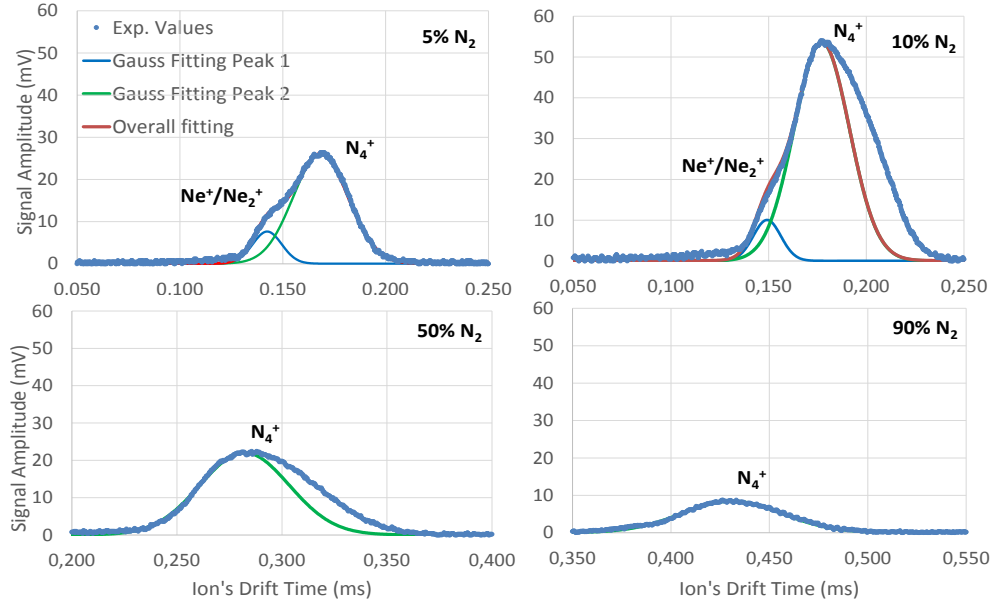
Figure 1. Time-of-arrival spectra averaged over 128 pulses for several Ne-N_2 mixtures (5%, 10%, 50% and 90% of N_2) at a pressure of 8 Torr, temperature of 298 K and for a reduced electric field of 15 Td with a voltage across GEM of 23 V (background noise subtracted).

Table 1. Summary of possible reactions and respective rate constants or cross section for electron impact ionization of the different primary ions for 23 eV.

Reaction	Rate Constant	Cross section (23 V)	Ref.
$e^- + Ne \rightarrow Ne^+ + 2e^-$	–	$0.0166\pm0.001\times10^{-16}$ cm^2	[17]
$Ne^+ + Ne \rightarrow Ne + Ne^+$	$3.4\pm0.85\times10^{-10}$ cm$^3\cdot$s^{-1}	–	[19]
$Ne^+ + 2Ne \rightarrow Ne_2^+ + Ne$	$4.4\pm0.4\times10^{-32}$ cm$^6\cdot$s^{-1}	–	[20]
$e^- + N_2 \rightarrow N_2^+ + 2e^-$	–	$0.492\pm0.025\times10^{-16}$ cm^2	[18]
$N_2^+ + N_2 + M \rightarrow N_4^+ + M$, (M = N_2)	$5.5\pm0.3\times10^{-29}$ cm$^6\cdot$s^{-1}	–	[21]
$N_2^+ + N_2 + M \rightarrow N_4^+ + M$, (M = Ne)	1.4×10^{-29} cm$^6\cdot$s^{-1}	–	[21]
$Ne^+ + N_2 \rightarrow N_2^+ + Ne$	$1.1\pm0.44\times10^{-13}$ cm$^3\cdot$s^{-1}	–	[19]

responsible for the peaks observed will be Ne ions (Ne^+/Ne_2^+)[1] for the peak with higher mobility and the N_4^+ ions for the peak with lower mobility. In this case the expected fraction of each species collected is about 83% of N_4^+, 8.9% of Ne^+ and 6.8% of Ne_2^+ and 1.3% of N_2^+, whereas the ions formed at the GEM are 78% N_2^+ and 22% Ne^+. Further increasing the concentration of N_2 in the mixture will lead mainly to the formation of N_4^+. Looking at figure 2b (50% N_2), at about 0.28 ms, the drift time of the ion responsible for the spectrum in figure 1 (50% N_2), the expected fraction of each ion species is 99.8% of N_4^+, with the remaining representing only 0.2%, while the ions formed at the GEM are 97% N_2^+ and 3% Ne^+.

---

[1]As can be see from figure 2a the conversion of Ne^+ to Ne_2^+ is incomplete for this mixture, so the mobility measured is in fact the result of the drift path travelled both as Ne^+ and Ne_2^+.
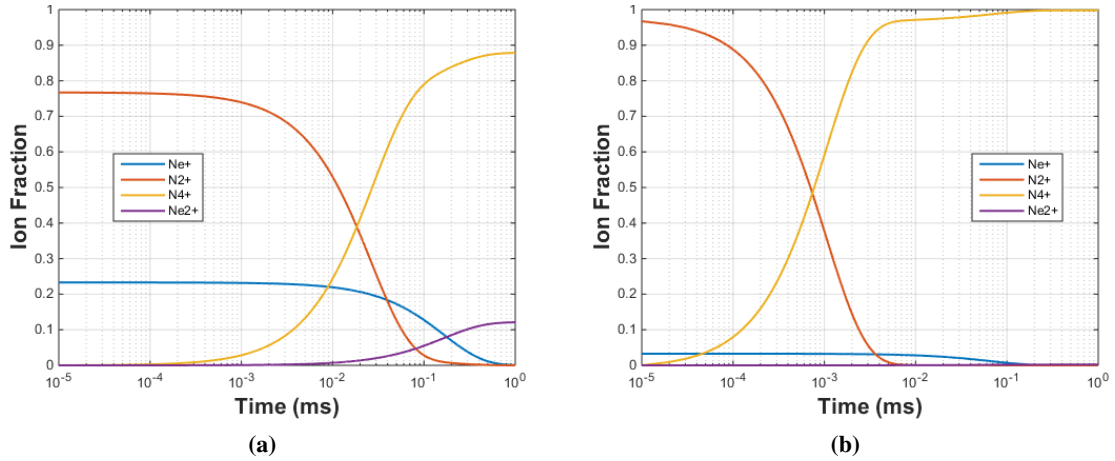
Figure 2. Fraction of ions that can be formed as a function of time for Ne-N_2 mixtures of 10% (a) and 50% (b) of N_2, for a total pressure of 8 torr.

In fact, above 10% N_2 the only ion expected is N_4^+ which results from N_2^+ through a three-body reaction:

$$N_2^+ + N_2 + M \rightarrow N_4^+ + M \tag{3.1}$$

where M is an atom or molecule from the gas mixture, in our case Ne or N_2. In this collision the excess energy is removed by a third body (M), preventing its dissociation back to N_2^+. As can be seen from table 1 the reaction time will depend on M. As a consequence the reaction time for the formation of N_4^+ will be affected by the chosen reaction partner (M), which can affect the signal shape if the drift time is of the same order of magnitude of the reaction time. A longer reaction time means that part of the drift path is spent as N_2^+, which has lower mobility than N_4^+, originating an asymmetry towards the right side of the N_4^+ peak, as can be observed in the drift spectra displayed in figure 1.

As for the N_2^+ ion, it can be originated either from direct electron impact ionization of N_2 or from the charge transfer reaction,

$$Ne^+ + N_2 \rightarrow N_2^+ + Ne \tag{3.2}$$

that has a lower reaction time than the competing one,

$$Ne^+ + 2Ne \rightarrow Ne_2^+ + Ne \tag{3.3}$$

in the pressure conditions of this experiment (as can be seen in figure 2b for 50% of N_2). Since to our knowledge there is no charge transfer between Ne_2^+ and N_2 we expect that, once formed, it will remain unaltered through the drift distance. Also, since the dissociation energy of N_4^+ (0.87 eV) is much larger than the kinetic energy of the ion under low reduced electric field, once N_4^+ is formed it will have a low probability of dissociating back into N_2^+ and N_2 [6].

Concerning the peak area, we can observe in figure 1 that it varies with N_2 concentration in the mixture, a feature somehow related to the availability of Ne. There is also a peak shift to lower drift times with decreasing N_2 concentration, which translates into an increase in the ion mobility.

This increase is due to the fact that the Ne atom has a much smaller mass than N_4^+ ion implying a much lower energy loss in elastic collisions with the gas atoms/molecules.

As mentioned, Blanc's law can be used to predict the mobility of the ions in gaseous mixtures. In figure 3 we plot the inverse of the reduced mobility obtained for the ions produced in the Ne-N_2 mixture as a function of the different mixture ratios studied for a pressure of 8 Torr and for E/N of 15 Td, at room temperature (298 K).
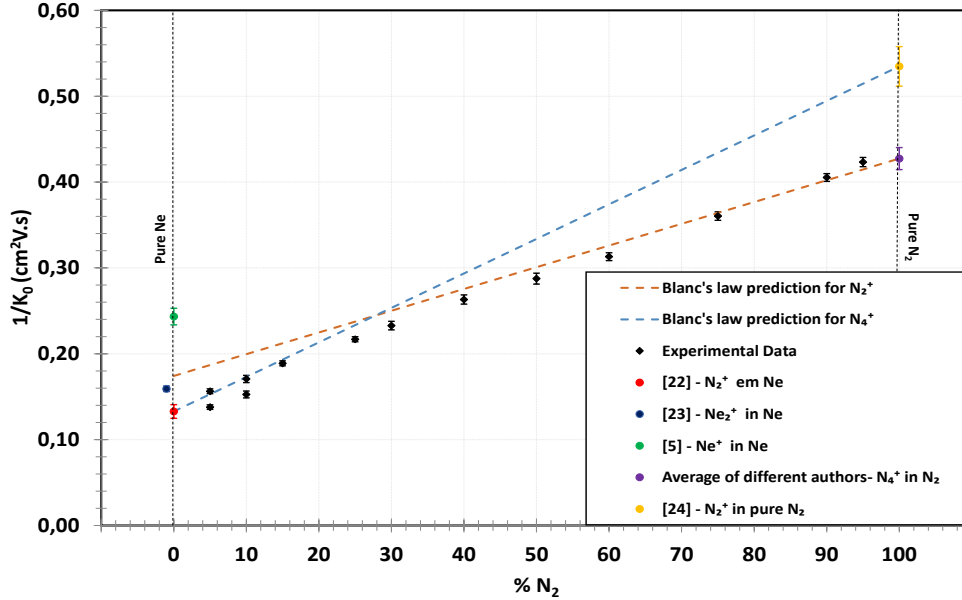

Figure 3. Inverse of the reduced mobility of the ions produced in the Ne-N_2 mixture for a pressure of 8 Torr and for a E/N of 15 Td at room temperature. The dotted lines represent the mobility values expected from Blanc's law for N_4^+ (orange) and for N_2^+ (blue).

Dashed lines representing Blanc's law for the most abundant ion, N_4^+ (orange), as well as for N_2^+ (blue) are also displayed. In this case, in Blanc's law (eq. (1.4)), K_{g1} and K_{g2} were obtained either by using Langevin's formula (eq. (1.3)) for $K_{(N_2^+/Ne)}$ or by selecting experimental values from literature.

Observing figure 3 it is possible to conclude that the ion mobility experimentally obtained roughly follows, within error bars, Blanc's law for the most abundant ion down to 40% N_2, while below this N_2 concentration it deviates towards the N_2^+ theoretical value given by Blanc's law. The same figure indicates that the ion species observed depends on the amount of N_2 in the mixture (a second peak appears as seen in figure 1 for 5% and 10% N_2 and also in figure 3).

In fact, starting from pure Ne, as a result of the reaction rates and pressures, we have initially the formation of Ne^+ and Ne_2^+, then Ne^+ and N_4^+ and finally only N_4^+ according to the different reaction channels discussed previously. In addition it is also possible to see that increasing N_2 leads to a significant decrease in the mobility of the N_2 ions present, i.e. N_4^+.

The mobility values in this experiment range from 6.41±0.06 to 2.37±0.03 cm^{2}V^{-1}s^{-1} for the slowest ion, and from 7.20±0.06 to 6.55±0.05 cm^{2}V^{-1}s^{-1} for the fastest ion, for E/N = 15 Td and 8 Torr. No significant variation of the mobility was observed in the range of pressures (6–8 Torr) and of E/N (10–20 Td) studied.

The mobility values of the ions observed for the Ne-N$_2$ mixture ratios studied, at E/N of 15 Td, pressure of 8 Torr and at room temperature (298 K) are summarized in table 2.

Table 2. Mobility of the ions observed for the Ne-N$_2$ mixture ratios studied, obtained for E/N of 15 Td, at 8 Torr and 298 K.

Ne-N$_2$ Mixture	Mobility (cm^{2}V^{-1}s^{-1})	Mobility (cm^{2}V^{-1}s^{-1})
% of N$_2$	N$_4^+$	Ne$^+$/Ne$_2^+$
5%	6.41 ± 0.06	7.20 ± 0.06
10%	5.86 ± 0.05	6.55 ± 0.05
15%	5.30 ± 0.05	–
25%	4.61 ± 0.06	–
40%	3.80 ± 0.05	–
50%	3.46 ± 0.08	–
60%	3.19 ± 0.06	–
75%	2.78 ± 0.04	–
90%	2.47 ± 0.03	–
95%	2.37 ± 0.03	–

From 0 to 100% N$_2$, the peaks observed were seen to vary in position and area, demonstrating that the ion or ions formed and their mobilities depend on the ratio of the two gases used.

4   Conclusion

In the present work we measured the reduced mobility of ions originated by electron impact in the Ne-N$_2$ mixtures using pressures from 6 to 8 Torr, low reduced electric fields (10–20 Td) and different mixture ratios. The experimental results show that for the mentioned mixtures two peaks were observed in the range of concentrations studied. The ions responsible for these peaks are believed to be the ones originated in Ne (Ne$_2^+$ and Ne$^+$) for concentrations of N$_2$ up to 5% while for concentrations up to 10% of N$_2$, the ions observed are Ne$^+$ and N$_4^+$. Above 10% N$_2$ the only ion observed is N$_4^+$, which can be formed through different reaction channels. The ions' mobility was seen to decrease with the increase of N$_2$ concentration in the mixture with the behaviour following roughly, Blanc's law for N$_4^+$ down to 40% N$_2$ and then gradually changing towards the N$_2^+$ predicted behaviour. An asymmetry was observed in some spectra, this asymmetry is expected to be due to the different reaction paths discussed and that originate N$_4^+$.

Additionally we verified that the mobilities calculated did not display a significant dependence either with pressure in the pressure range studied (6–8 Torr), or with E/N in the range used in this work (10–20 Td).

Future work is expected with other gaseous mixtures. It is our intention to extend the work on ion mobility using different mixtures of known interest such as Xe-CO$_2$, Xe-CH$_4$, Ar-CF$_4$, Ne-CF$_4$ and Xe-CF$_4$.

Acknowledgments

References

[1] W. Blum and L. Rolandi, *Particle Detection with Drift Chambers*, Springer-Verlag, Berlin, Germany (1994).

[2] G.F. Knoll, *Radiation detection and measurements*, John Wiley and Sons Inc., New York, U.S.A. (2000).

[3] G.A. Eiceman, Z. Karpas and H.H.J. Hill, *Ion Mobility Spectrometry*, third edition, CRC Press-Taylor & Francis Group (2014).

[4] P.N.B. Neves, C.A.N. Conde and L.M.N. Távora, *Experimental measurement of the mobilities of atomic and dimer Ar, Kr and Xe ions in their parent gases*, *J. Chem. Phys.* **133** (2010) 124316.

[5] P.N.B. Neves, A.N.C. Garcia, A.M.F. Trindade, J.A.S. Barata, L.M.N. Távora and C.A.N. Conde, *Experimental measurement of the Ne^+ and Ne_2^+ mobilities in Ne and the reaction rate coefficient for $Ne^+ + 2Ne \rightarrow Ne_2^+ + Ne$*, *IEEE Trans. Nucl. Sci.* **58** (2011) 2060.

[6] A.N.C. Garcia, P.N.B. Neves, A.M.F. Trindade, F.P. Santos and C.A.N. Conde, *A new contribution to the experimental measurement of the N_4^+ and N_2^+ ion mobility in N2 at 298K*, 2012 *JINST* **7** P02012.

[7] A.F.V. Cortez et al., *Experimental measurement of the mobility of ions originated in ethane in their parent gas*, 2013 *JINST* **8** P07013.

[8] A.F.V. Cortez et al., *Experimental measurements of the mobility of methane ions in Ar-C_2H_6*, 2013 *JINST* **8** P12012.

[9] A.N.C. Garcia, P.N.B. Neves, A.M.F. Trindade, A.F.V. Cortez, F.P. Santos and C.A.N. Conde, *Experimental ion mobility measurements in Xe-N2 mixtures*, 2014 *JINST* **9** P07008.

[10] A.M.F. Trindade et al., *Experimental study on ion mobility in Ar-CH_4 mixtures*, 2014 *JINST* **9** P06003.

[11] P.M.C.C. Encarnação et al., *Experimental Ion Mobility measurements in Ar-CO_2 mixtures*, 2015 *JINST* **10** P01010.

[12] Y. Kalkan, M. Arslandok, A.F.V. Cortez, Y. Kaya, İ. Tapan and R. Veenhof, *Cluster ions in gas-based detectors*, 2015 *JINST* **10** P07004.

[13] P.M.C.C. Encarnação et al., *Experimental Ion Mobility measurements in Ne-CO_2 and CO_2-N_2 mixtures*, 2016 *JINST* **11** P05005.

[14] P. Langevin, *Une formule fondamentale de théorie cinetique*, Ann. Chim. Phys. **5** (1905) 245.

[15] E.A. Mason and E.W. McDaniel, *Transport Properties of Ions in Gases*, John Wiley and Sons Inc., New York, U.S.A. (1988).

[16] A. Blanc, *Recherches sur le mobilités des ions dans les gaz*, *J. Phys. Theor. Appl.* **7** (1908) 825.

[17] D. Rapp and P. Englander-Golden, *Total Cross sections for Ionization and Attachment in Gases by Electron Impact. I. Positive Ionization*, *J. Chem. Phys.* **43** (1965) 1464.

[18] Y. Itikawa, *Cross sections for Electron Collisions with Nitrogen Molecules*, *J. Phys. Chem. Ref. Data* **35** (2006) 31.

[19] V.G. Anicich, *Evaluated Bimolecular Ion-Molecule Gas Phase Kinetics of Positive Ions for Use in Modeling Planetary Atmospheres, Cometary Comae, and Interstellar Clouds*, *J. Phys. Chem. Ref. Data* **22** (1993) 1469.

[20] A.P. Vitols and H.J. Oskam, *Reaction rate constant for $Ne^+ + 2Ne \rightarrow Ne_2^+ + Ne$*, *Phys. Rev.* **A 5** (1972) 2618.

[21] P.A.M. van Koppen et al., *Ion-molecule association reactions: A study of the temperature dependence of the reaction $N_2^+ + N_2 + M \rightarrow N_4^+ + M = N_2$, Ne, and He: Experiment and theory*, *J. Chem. Phys.* **81** (1984) 288.

[22] Y. Kondo and J.L. Moruzzi, *Mobilities of O_2^+, N_2^+ and CO^+ in Ar, Ne and Kr*, *Int. J. Mass Spectrom. Ion Phys.* **38** (1981) 1.

[23] O.J. Orient, *Mobility of mass-identified ions in neon and reaction rate coefficient for $Ne^+ + 2Ne \rightarrow Ne_2^+ + Ne$*, *Chem. Phys. Lett.* **23** (1973) 579.

[24] J.T. Mosley et al., *Mobilities, diffusion coefficients, and reaction rates of mass-identified nitrogen ions in nitrogen*, *Phys. Rev.* **A 178** (1969) 240.